

Fast Switchable Micro-Lenticular Lens Arrays Using Highly Transparent Nano-Polymer Dispersed Liquid Crystals

Srinivas Pagidi, Ramesh Manda, Surjya Sarathi Bhattacharyya, Sung Guk Lee, Seong Min Song, Young Jin Lim, Joong Hee Lee, and Seung Hee Lee*

A polarization-dependent micro-lenticular lens array (MLA) based on phase modulation of the nanostructured polymer dispersed liquid crystal (nano-PDLC) is proposed. The transparent and optically isotropic composite is formed by photo-polymerization induced phase separation of the LC and pre-polymer mixture. The gradient field is generated by interdigitated electrodes and the LCs in nanosized droplets in nano-PDLC orient along the field direction, resulting in field-induced birefringence from the optically isotropic phase. Consequently, the MLAs are formed at the focal plane, in which its measured focal length is 22 μm at 50 V_{rms} . Besides, the position of focused beam in MLA device can be tuned depending on the polarization direction of an incident beam. The MLA device can realize a 3D image when the polarized 2D image arrays encounter the microlens. The proposed MLA device can pave the way toward upcoming fast switchable 2D/3D display device applications with a very fast switching time of 3.8 ms.

the lower driving voltages. However, the parallax barrier reduces transmittance to half, causes resolution loss and limits viewing angles due to slits in front of the display panel and the flat-type lenticular lens are not switchable. Furthermore, the switchable lenticular lens which utilizes nematic LC requires large cell gap to achieve enough periodic phase modulation between the adjacent electrodes for realizing the lensing effect, which results in slow switching response time in conventional devices with pure nematic LC. Besides, the quality of displayed image becomes distorted when the externally applied force is strong enough. Therefore, further investigations are required to achieve switchable LC lens with fast response time and a mechanical shock

resilient network, which could satisfy the future demands of electronic devices with flexibility and bendability.

Contrary to shortcomings of traditional modes, a binary composite of the optically isotropic liquid crystal (OILC) was introduced. Currently, there are two types of binary composites attracting liquid crystal display industrial research, one is nanostructured polymer dispersed liquid crystals (nano-PDLCs) and the other is the polymer-stabilized blue phase (PSBP). The great advantages of OILCs are resilience to external pressures, optically isotropy in the field-off state, wide viewing angle, cell gap independence, alignment layer-free, and rubbing-free allows simplification of device fabrication.^[5–8] In addition, OILC exhibits fast switching times.^[9–12] Owing to these revolutionary benefits many potential users became fascinated by OILCs.


In addition, the nano-PDLC is a composite consisting of low molecular weight prepolymer and the LC. Optimized UV light intensity and materials, and concentration ratio of monomer to LC under ambient conditions result in the nanosized LC droplets encapsulated by polymer network viz., nano-PDLC in which the droplet size is smaller than the wavelength of visible light.^[8,12] In addition, the random orientation of the LC director results in the optically isotropic phase so that the nano-PDLC exhibits excellent black state under the crossed polarizers. On the other hand, the PSBP also shows an optically isotropic phase with very fast electro-optic response. However, temperature sensitive phase separation and high hysteresis are hindering their extensive industrial applications.^[7,13,14] Utilizing the benefits of OILCs, several photonic devices including polarization independent tunable microlens,^[15–17]

1. Introduction

During last few decades, field switchable adaptive lenses using liquid crystals (LCs) have extensively gained much popularity in developing numerous applications including biometrics, imaging, displays, and beam steering devices. Contemporary research in the field of liquid crystals engrossed significant importance on eye-glass free switchable 2-dimensional (2D) and 3-dimensional (3D) auto-stereoscopic lens to realize vivid images with depth of field. In conventional 2D/3D modes, the parallax barriers,^[1,2] and lenticular lens,^[3,4] are predominantly utilized, owing to their compact size, light weight, and

S. Pagidi, Dr. R. Manda, S. G. Lee, S. M. Song, Dr. Y. J. Lim, Prof. J. H. Lee, Prof. S. H. Lee
 Applied Materials Institute for BIN Convergence
 Department of BIN Convergence Technology Chonbuk National University
 Jeonju 54896, Republic of Korea
 E-mail: lsh1@chonbuk.ac.kr

Dr. S. S. Bhattacharyya
 Asutosh College
 Department of Physics
 92, Shyamaprasad Mukherjee Road, Kolkata 700 026, West Bengal, India
 Prof. S. H. Lee
 Department of Polymer-Nano Science and Technology
 Chonbuk National University
 Jeonju 54896, Republic of Korea

 The ORCID identification number(s) for the author(s) of this article can be found under <https://doi.org/10.1002/admi.201900841>.

DOI: 10.1002/admi.201900841

diffraction gratings,^[18,19] etc. were developed. When compared with conventional LC display and photonics with pure nematic LC, OILCs with PSBPs and nano-PDLCs can be considered as the candidate for fabrication of fast switchable 2D display and photonic devices such as tunable lens and diffractors.

In this paper, we have proposed switchable micro-lenticular lens arrays (MLAs) utilizing phase modulation of the optically isotropic nano-PDLCs. The homogeneous mixture was phase separated using the well-known method of polymerization-induced phase stabilization. On field-on state, the phase retardation is induced by reorientation of LC director encapsulated in the polymer network; therefore, the optical path follows the gradient refractive index, resulting in realization of MLAs. Besides, the position of focused beam in MLA device can be changed depending on the polarization state of the incident beam. Finally, a 3D image can be realized when the incident linearly polarized light encounters MLAs.

2. Switching Mechanism of the Micro-lenticular Lens Arrays

The cross-sectional structure of the proposed polarization-dependent switchable MLA device with nano-PDLC is schematically depicted (Figure 1). The bottom substrate has interdigitated electrodes with electrode width (w) of $4\ \mu\text{m}$ and gap (l) between them, $4\ \mu\text{m}$ is shown in Figure 1a, and a top glass substrate was attached with a cell gap of $10\ \mu\text{m}$. As indicated in Figure 1b, the polymer encapsulated LC droplets with size less than $200\ \text{nm}$ do neither scatter the incident light nor contribute to any

optical phase change because the director of each individual LC droplet is oriented in random in comparison with neighboring LC droplets in absence of the applied field. Therefore, the nano-PDLC exhibits an optically isotropic phase, i.e., efficient black state under the crossed polarizers having a refractive index n_i expressed as $n_i = v_p n_p + v_{lc} n_{avg}$, where v_p and v_{lc} are the filling factor of polymer and LC in the composite, n_p and n_{avg} is the refractive index of the polymer and average refractive index of the LC satisfying the condition $n_p < n_{avg}$.^[20] Since $n_{avg} = (2n_o + n_e)/3$, where n_o and n_e is the ordinary and extraordinary refractive indices of the LC, it is larger than n_p so that the magnitude of n_i is between the n_p and n_{avg} . On the other hand, at field-on state, the LC director encapsulated in the polymer matrix preferably reorients along the gradient field, resulting in the formation of the graded-index in the induced birefringence.

In the proposed device, three different refractive indices at three different positions (I: above the electrode, III: the center of the gap between the pixel and common electrodes, II: the space between above electrodes (region I) and gap center (region III)) could be considered, as indicated in Figure 1b. At region I, the intensity of the in-plane electric field remains minimum above the pixel and common electrodes compared to the other two regions II and III. Thus preferable random orientation of LC directors prevails above the pixel and common electrodes. Hence, the ray propagating through in the region I will experience effective refractive index n_i . At region II, high intensity of oblique electric field near the edge of the pixel and common electrode imparts splay-bend deformation over randomly oriented LC molecules to preferably have LC director nearly in an oblique direction. Consequently, the

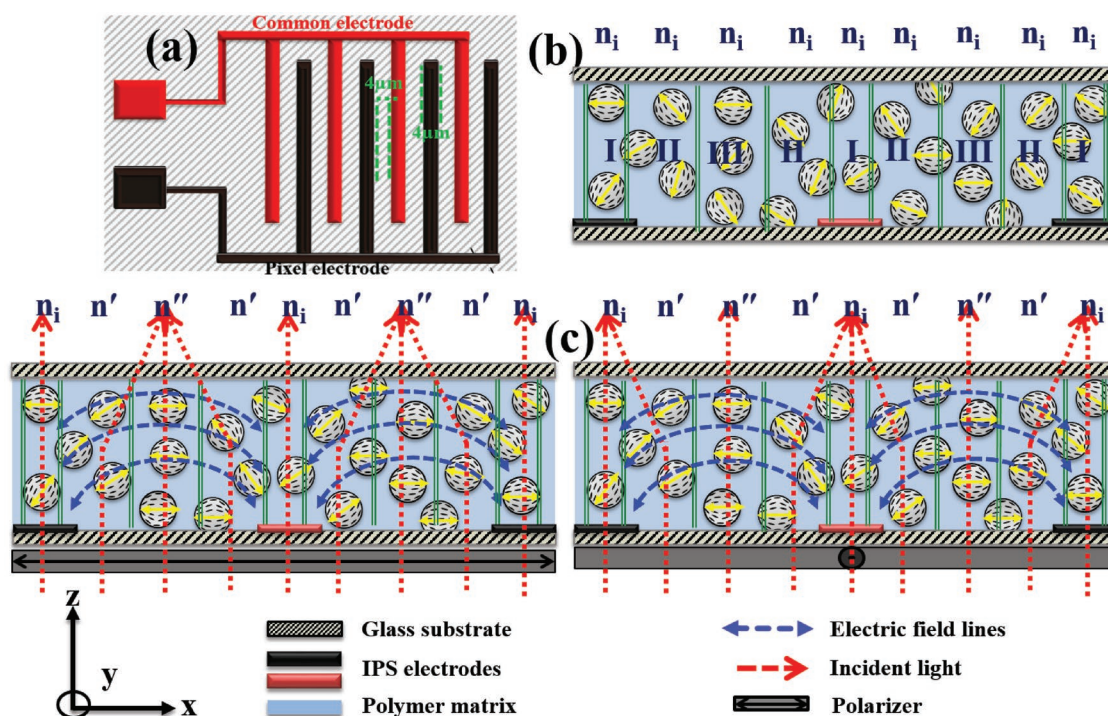


Figure 1. Micro-lenticular lens arrays using nanostructured LC droplets and its switching mechanism. a) Top view of the electrodes, b) Random orientation of LC directors in the field-off state, and c) Focused beam position in micro-lenticular arrays depending on the polarization direction of an incident beam in the field-on state.

propagating polarized beam would experience effective refractive index n' , which can be defined as $n' \sim v_p n_p + v_{lc} n_{eff}$ where $n_{eff} = \frac{n_o n_e}{\sqrt{n_o^2 \cos^2 \theta + n_e^2 \sin^2 \theta}}$ where θ is the angle between LC director and the polarization of the incident light, so that its value depends on both polarization direction of an incident beam and angle of LC director with respect to vertical direction. When a polarized direction of an incident beam is parallel to the electrode direction, $n_{eff} > n_o$, so n' will be n_o' , whereas the polarization direction of the beam is perpendicular to the electrode direction, so n' will be n_e' . Moving the position from II to III, the intensity of the oblique electric field gradually reduces and the in-plane field dominates. Besides, the symmetric arrangement of the consecutive pixel and common electrode gives rise to symmetric distribution of electric field lines causing a continuous modulation in the LC director profile. At position III, the effective refractive index n'' can be defined as $n'' \approx v_p n_p + v_{lc} n_{eff}$ again; in which n_{eff} can be replaced by n_o (n_e) when polarization direction of an incident beam is parallel (perpendicular) to the in-plane field direction and thus n'' can be either n_e'' or n_o'' depending on polarized direction of an incident beam. Consequently, when a polarized direction of an incident beam is perpendicular to the electrode direction, it experiences n_i , n_e' , and n_e'' in the region I, II, and III, respectively, whose magnitude follows this order $n_i < n_e' < n_e''$. Now, when the polarization direction of the beam is rotated by 90° , it experiences n_i , n_o' , and n_o'' in the region I, II, and III, respectively, whose magnitude follows this order $n_i > n_o' > n_o''$. This implies, the incident beam is almost undeviated while propagating through above electrodes; however, encountering graded-index between the pixel and common electrodes undergoes deviates from incident direction while passing through the electric field modulated refractive index profile of polymer encapsulated LC director. Such electric field induced periodic deformation of polymer encapsulated LC director between the periodic pixel and common electrode, in turn, induces plano-concave lensing effect over the incoming transmission beam and also modulates the polarization state of emergent beam depending on the polarization state of the incident beam. Therefore, the effective optical phase modulation is switched by the incident polarization considered as a polarization-dependent micro-lenticular lensing effect of the IPS device as depicted in Figure 1c.

In nano-PDLCs, when the electric field is applied, the LC with positive dielectric anisotropy in droplets encapsulated by the nanostructured polymer can align along the field direction, resulting in an induced birefringence (Δn_{ind}).^[21] The magnitude of Δn_{ind} associated with field-induced reorientation of LC inside droplets is expressed as Kerr effect $\Delta n_{ind} = K \lambda E^2$,^[18,22] where K is the Kerr constant, λ is the wavelength of the incident light, and E is the applied field. Furthermore, the optical phase difference ($\Delta \delta$) between the region I and III while the incident beam perpendicular to electrodes could be expressed as^[18,23]

$$\Delta \delta = \frac{2\pi}{\lambda} \left| \int_0^d n''(E) dz - n_i d \right| \quad (1)$$

where d is the cell gap. The focal length of the lenticular lens can be written as^[4,15]

$$f = \frac{\pi w^2}{4\lambda(\Delta \delta)} \quad (2)$$

where w is the width or pitch of the lenticular aperture and $\Delta \delta$ is the phase change measured between the lens centers to the edge of the electrode. The maximum $\Delta \delta$ equals to $\delta \phi$ which is defined as $\delta \phi = k \cdot d \cdot v_{lc} \cdot (n_e - n_o)/3$, where k is the wave vector ($2\pi/\lambda$) and v_{lc} is the filling factor defined as the ratio of the area occupied by polymer encapsulated LC droplets to the area of the sample explored via field emission scanning electron microscope (FE-SEM) image.^[16]

3. Results and Discussion

The polarizing optical microscopic images representing the switching dynamics of the micro-lenticular nano-PDLC captured at room temperature in the ambient conditions^[8,12] is depicted in Figure 2. In field-off state, the MLA device with polymer encapsulated LC director exhibit an excellent dark state in all three regions and the darkness remains invariant with the rotation of sample plane between crossed polarizers. Hence, the LC directors in nano-PDLC do not induce any phase retardation for a polarized incident beam, as shown in Figure 2a. However, the inevitable feeble optical scattering was observed in the device owing to mismatching of the refractive indices between interfaces of LC and polymer matrix and few larger droplets in the composite.^[24,25] On the other hand, to observe the induced birefringence, the device is placed between crossed polarizers while making an angle 45° between the polarization direction of an incident beam and electrode direction. When the electric field is applied to the interdigitated electrodes, the LC directors encapsulated in polymer droplets between the pixel and common electrodes reorient parallel to the field direction, giving rise to bright fringe patterns observed in the regions II and III. However, the region I remain dark because the intensity of the fringe electric field to reorient the LC directors is not enough. Consequently, the graded transmission intensity in the regions I, II, and III is observed and remains invariant even increasing the field strength as shown in Figure 2a. On-field withdrawal, the bright state goes back to the dark state very quickly without showing any residual birefringence and electro-optic hysteresis, unlike PSBPs.^[14] This could be due to the strong anchoring between interfaces of the LC and polymer matrix.

Figure 2b illustrates the change in position of focused beam in MLAs depending on the polarization direction of an incident beam. First, to observe focused MLAs, the analyzer is removed, and the polarization direction of an incident beam is adjusted perpendicular to electrode direction. In this condition, the optical paths for three different regions I, II, and III experience three different effective refractive indices n_i , n_e' , n_e'' with the order $n_i < n_e' < n_e''$, resulting in periodically focused MLAs in the region III at the focal plane, which perfectly matches with theoretical position described in the switching principle. The experimentally measured focal length of the proposed MLA device is $22 \mu\text{m}$ at $50 V_{rms}$. The calculated focal length with parameters $\lambda = 0.633 \mu\text{m}$, $d = 10 \mu\text{m}$, $v_{lc} = 0.179$, $\delta \phi = 0.45\pi$ radians, and $w = 4 \mu\text{m}$ is about $\approx 15 \mu\text{m}$, which is in a good

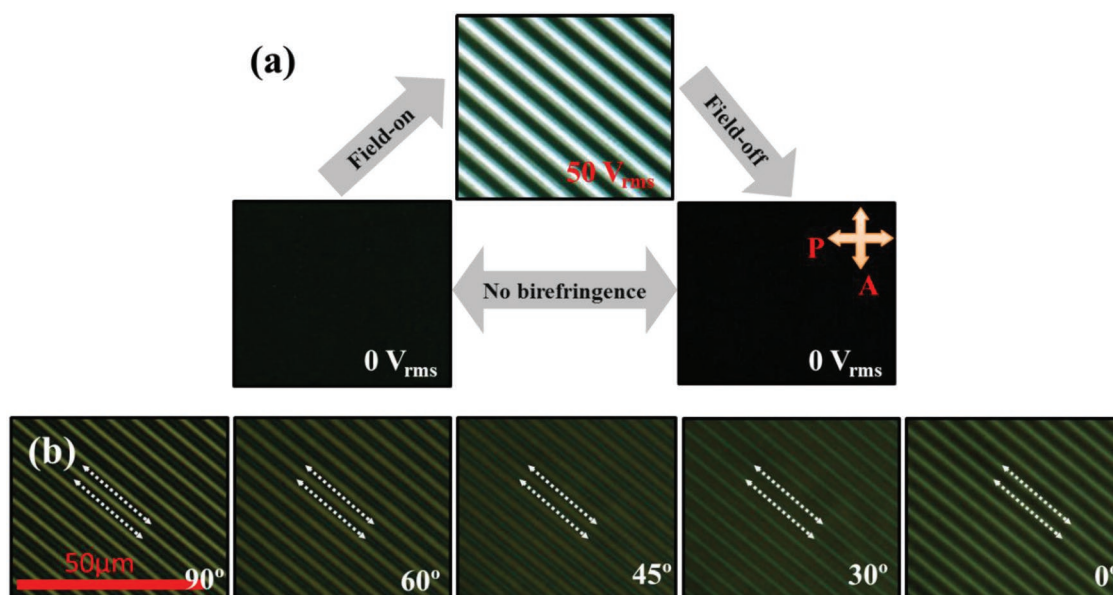


Figure 2. POM images showing optical switching of the micro-lenticular nano-PDLC device. a) $V = 0$ and $50 V_{rms}$ with the applied square wave frequency of 1 KHz, in which the dark image in the field-off state turns to a bright state only between electrodes in the field-on state. b) Focused beam positions change with polarization direction of an incident beam with respect to electrodes such that position of them changes from region III to region I as the angle changes from 90° to 0° .

agreement with the experimental result. The focal length mainly relies on the filling factor, the birefringence of LC, cell gap, and width of the lenticular pitch so that adjusting the first two parameters would obtain desired focal lengths. Second, the polarization direction of the incident beam was rotated from 90° to 0° with respect to electrode direction. Then, the maximum intensity of the focused beam in the region III gradually decreases to a minimum and increases to a maximum in the region I, as shown in Figure 2b. This confirms the incident polarized beam experiences the effective refractive indices in the order $n_i < n_e' < n_e''$ to $n_i > n_o' > n_o''$ in the regions I, II, and III, respectively, when the polarization direction is rotated by 90° . It is worthwhile to mention that the relative change in position of the focused beam between the region III and region I with respect to incident polarization direction strongly emphasize the proposed device is working as a polarization dependent micro-lenticular lens.

Figure 3a depicts the schematic array diagram of the 2D/3D switchable display prepared by assembling the proposed micro-lenticular nano-PDLC device on the 2D liquid crystal display (LCD). Each microlens formed between pixel and common electrodes of the MLA device covers two pixels of the LCD, i.e., left and right pixel and 2D to 3D image can be realized by switching MLA. In our studies, the polarized incident beam coming from the MLA device is unaffected, in field-off state, owing to the optically isotropic nano-PDLC phase. Therefore, a well-resolved clear 2D image is realized by the right and left eyes in all possible directions. In field-on state, it works as MLA so that the incident beam coming from the right and left pixel arrays encounter interface of the gradient refractive indices and hence deviates toward the left and right eyes, respectively, exhibiting duplicate images in the horizontal direction. In this test, the polarization direction of the LCD is in a

diagonal direction so that the duplicate image will occur in that direction. As indicated in Figure 3b,c, the text and the moving images coming from 2D LCD is unaffected by the MLA in field-off state but the images become duplicate in the diagonal direction at the applied voltage of 50 V, exhibiting feasibility of electrical switching from 2D to 3D by the proposed MLA without affecting much transparency of 2D LCD. Conclusively speaking, the proposed approach could realize a 3D image without using any special 3D glasses. Similarly, when the United States Air Force-1951 (USAF-1951) resolution target and the MLA device are in contact with one another, the USAF-1951 image appeared as a blurred and stretched in the horizontal direction, as shown in Figure 3d. The expansion of the object image in the horizontal direction exhibits a microlenticular lens effect of the device. A similar kind of results was reported with PVC/DBP gel,^[26] PNLC,^[27] and PVC gel,^[28] microlenses. In our case, the proposed micro-lenticular lens pitch is very short so that it can be applied to very high-resolution short pitch display like virtual displays or can adjust the micro-lenticular lens pitch according to the resolution of the display.

Figure 4a illustrates the experimental setup for measuring the electro-optical switchable responses of the MLA device. The relative transmittance intensity change was recorded with a photodetector and the corresponding data were collected using the oscilloscope when field-on and -off switching are performed. Herein, the switching-on and -off response is defined as the time taken for 10% to 90% transmittance change while applying and 90% to 10% while releasing the applied field, respectively, when the MLA is the position under crossed polarizers. Figure 4b depicts the measured switching-on and -off times of the proposed MLA device is 0.99 and 2.8 ms, respectively, faster than any previously reported nematic LC lens. In nano-PDLCs, the switching-on time is mainly attributed to the

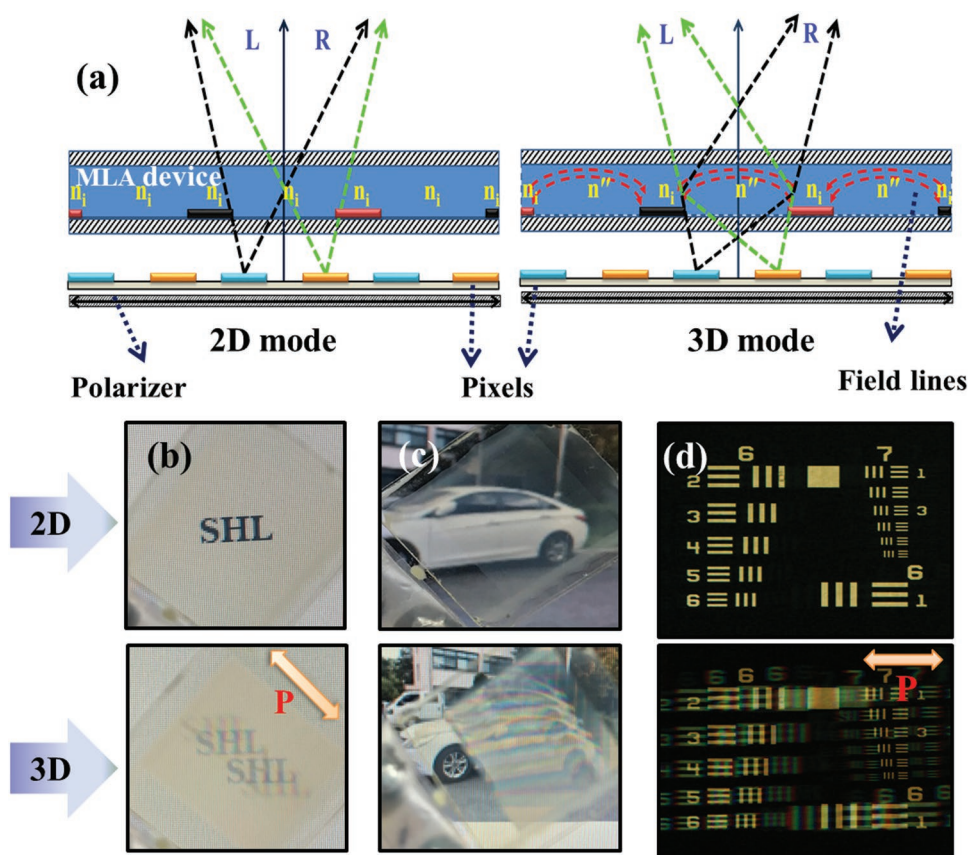


Figure 3. a) Schematic arrays diagram of the 2D/3D switchable display with proposed micro-lenticular nano-PDLC device. b,c) Photographic 2D at $V = 0 V_{rms}$ and 3D at $V = 50 V_{rms}$ of the static text “I” and moving images while the MLA device placed on the 2D LCD panel, and d) Optical images of the USAF-1951 resolution target observed through the MLA device.

magnitude of the applied field, however, the switching-off time (τ_{off}) time could be expressed as^[29]

$$\tau_{off} = \frac{\gamma_1 R^2}{k_{eff} W_s (2\pi)^2} \quad (3)$$

where W_s is the surface anchoring energy between interfaces of the LC and polymer matrix, and k_{eff} is the effective elastic

deformation, which is resultant of splay k_{11} and bent k_{33} deformations. Besides, the τ_{off} is accompanied by the relaxation of the LC molecules in the polymer matrix, which is mainly relied on the viscoelastic constants (γ_1/k_{eff}) of the LC utilized. Generally, in nano-PDLC, the switching responses are faster as compared to the conventional LC modes because the LC droplets embedded in the polymer matrix are nanometer size as compared to the micrometer-size cell gap in nematic LC

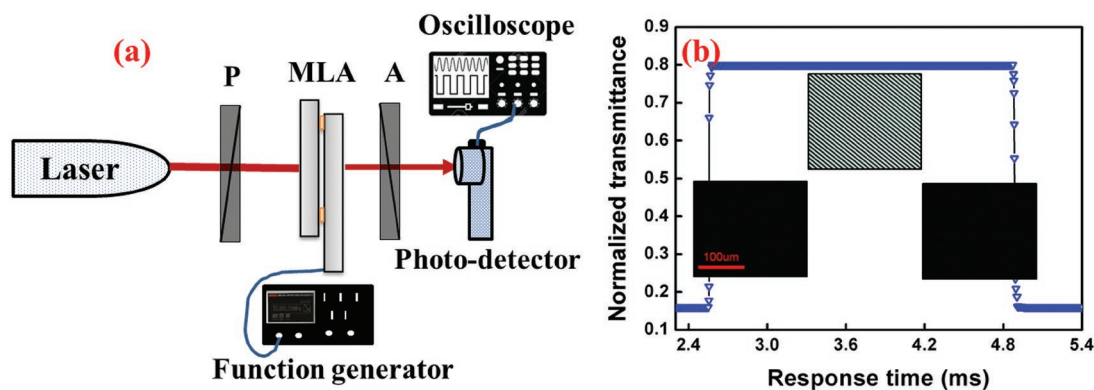


Figure 4. a) Experimental set-up for measuring the switching response time of the micro-lenticular device. b) Response time measured with a constant square wave voltage of $60 V_{rms}$ at 1 kHz and inset is the polarized optical images.

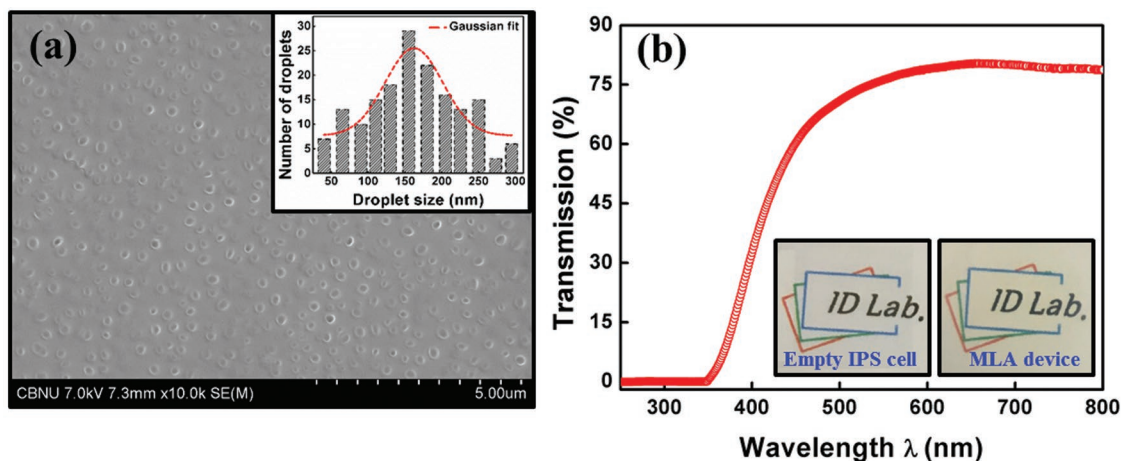


Figure 5. a) FE-SEM images of the LC removed polymer matrix and the inset is droplet size distribution with Gaussian fit, and b) UV-vis transmission spectrum and the inset photographic images of the micro-lenticular device and empty IPS cell above characters.

lens. Therefore, the LC droplet exerts very strong anchoring energy owing to an increased ratio of the effective surface area to the effective volume within the droplet. The reorientation switching mechanism of the nanostructured LC droplet was clearly elucidated and reported in the literature.^[30] In addition, a few similar kinds of fast responses are reported in the literature.^[10,18,20] Furthermore, we can achieve much faster electro-optical switching times via increasing W_s or decreasing of R , however, it sacrifices an operating voltage of the device.

The surface morphology of the LC removed polymer microstructure was investigated using the FE-SEM. To perform the FE-SEM, the sample preparation was clearly explained in the literature.^[31] The microstructure of the polymer matrix and the relative droplet size distribution is illustrated in **Figure 5a**. Herein, the droplet size distribution is estimated using the ImageJ software (Java software, developed by the National Institute of Health). The Gaussian fit exhibits the estimated average size of the LC droplet is 165 nm with the filling factor (v_{lc}) of 17.9%. The microimage and droplet size distribution reveal that the LC droplets are uniformly distributed all over the polymer matrix, in which most of the droplet sizes are in the range of 50–220 nm below the wavelength of the visible regime ($R < \lambda$). Therefore, one could anticipate the film should

not generate much scattering and the three-dimensionally surrounded polymer matrix exerts strong anchoring to the LC, which explains transparency and fast switching time. Finally, the UV-vis transmittance spectrum was measured as a function of wavelength in the range of 300–800 nm as depicted in **Figure 5b**. The spectrum indicates that the transmittance at 400 nm is quite low and it increases with the increasing wavelength of the incident light since the incident light scatters more in the shorter wavelength regime of 400 nm due to few droplets with its size over 200 nm. The transmittance of the proposed MLA device at 630 nm is as high as $\approx 95\%$ when compared to the transmittance of the empty cell (see inset images for transparency comparison and the image is clearly visible in the proposed MLA device), which is much higher than that reported in the microlens using PDLC.^[32]

4. Conclusions

In summary, we have successfully demonstrated a polarization-dependent MLA device based on phase modulation of the optically isotropic nano-PDLC, in which the binary mixture was phase separated by exposing high intensity of UV light. The proposed

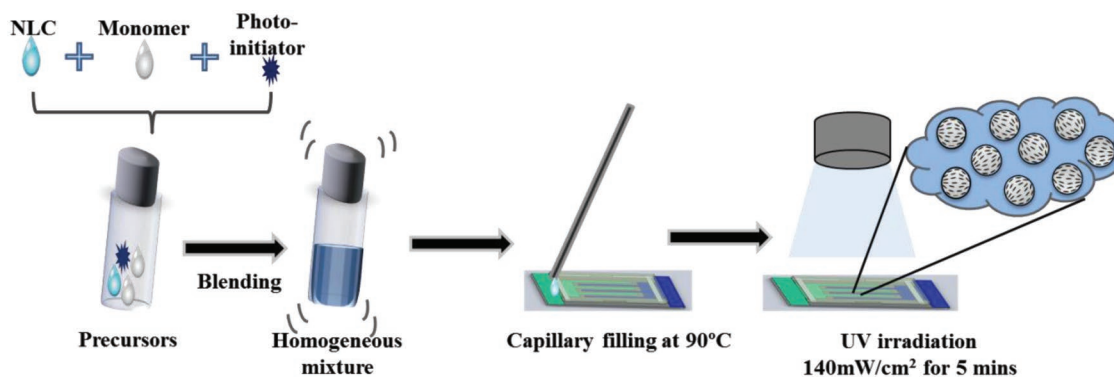


Figure 6. Schematic diagram for the preparation of the optically isotropic nanophase separated polymer dispersed liquid crystal droplets (nano-PDLC).

MLA device exhibits optically transparent in the wavelength of visible regime. The induced gradient refractive index by reorientation of the LC directors in the nano-PDLC driven by the field with interdigitated electrodes gives rise to enough optical path difference to form MLAs with the measured focal length of 22 μm in which the position of a focused beam depends on the polarization direction of the incident beam. Interestingly, the device can switch very fast with a response time of ≈ 1 ms from a transparent state to lenticular lens. The performances of the proposed optically isotropic MLA device become a potential candidate for the switchable 2D/3D flexible and photonic device applications.

5. Experimental Section

Materials and Preparation Procedure: The nano-PDLC composite was prepared using positive high dielectric anisotropy nematic liquid crystal mixture, MLC-2053 ($\Delta\epsilon = 42.6$, $\Delta n = 0.235$, and $T_{NI} = 86$ °C, from Merck Advanced Technology, Korea) and conventional thiolene based prepolymer NOA-65 (Norland Optical Adhesive, $n_p = 1.5122$ at 20 °C and 589 nm). A small amount of the photoinitiator (Irgacure-907) was added to the binary mixture to initiate the radical polymerization upon the UV exposure. The homogeneous mixture consists of nematic LC (42.5 wt%), NOA-65 (57.2 wt%), and photoinitiator (0.3 wt%). **Figure 6** depicts the schematic diagram for the preparation of the optically isotropic nano-PDLC.

Characterization Techniques: To investigate the various optical properties of the MLA device, several characterization techniques were performed. The polarizing optical microscope (POM) (Nikon, ECLIPSE E600, Japan) attached with charge coupled device camera (Nikon, DXM 1200), was used and the field was applied to the MLA device using a function generator (Agilent 33521A). The relative change in transmittance of the switching times was recorded using photodetector (Thor labs, DET36A/M, 350–1100 nm) and the data were collected using the oscilloscope (Tektronix, DPO2024B). The wavelength-dependent transmission spectrum was measured using the UV–vis spectroscopy (SCINCO, S-3100) from ultraviolet to near infrared region. The photographic images were taken using the high-resolution camera (Samsung, NX1000). Finally, the surface morphology of the polymer network was characterized using the FE-SEM.

Acknowledgements

This research was supported by the Basic Science Research Program through the National Research Foundation of Korea (NRF) funded by the Ministry of Education (2016R1A6A3A11930056 and 2016R1D1A1B01007189).

Conflict of Interest

The authors declare no conflict of interest.

Keywords

3D image, liquid crystals, micro-lenticular lens, optical device, polymer encapsulated nanostructured liquid crystal droplets

Received: May 13, 2019

Revised: June 20, 2019

Published online:

- [1] J. Flack, J. Harrold, G. J. Woodgate, *Proc. SPIE* **2007**, 6490, 64900M.
- [2] N. S. Holliman, N. A. Dodgson, G. E. Favalora, L. Pockett, *IEEE Trans. Broadcast.* **2011**, 57, 362.
- [3] M. P. Krijn, S. T. de Zwart, D. K. de Boer, O. H. Willemsen, M. Sluijter, *J. Soc. Inf. Disp.* **2008**, 16, 847.
- [4] H. Ren, S. Xu, Y. Liu, S. T. Wu, *Opt. Express* **2013**, 21, 7916.
- [5] N. Akamatsu, W. Tashiro, K. Saito, J. I. Mamiya, M. Kinoshita, T. Ikeda, J. Takeya, S. Fujikawa, A. Priimagi, A. Shichido, *Sci. Rep.* **2015**, 4, 5377.
- [6] M. S. Kim, Y. J. Lim, S. Yoon, S. W. Kang, S. H. Lee, M. Kim, S. T. Wu, *J. Phys. D: Appl. Phys.* **2010**, 43, 145502.
- [7] H. Kikuchi, M. Yokota, Y. Hisakado, H. Yang, T. Kajiyama, *Nat. Mater.* **2002**, 1, 64.
- [8] N. H. Park, S. C. Noh, P. Nayek, M. H. Lee, M. S. Kim, L. C. Chien, J. H. Lee, B. K. Kim, S. H. Lee, *Liq. Cryst.* **2015**, 42, 530.
- [9] S. W. Choi, S. I. Yamamoto, T. Iwata, H. Kikuchi, *J. Phys. D: Appl. Phys.* **2009**, 42, 112002.
- [10] J. H. Yu, J. J. Lee, Y. J. Lim, P. Nayek, S. Kundu, S. W. Kang, S. H. Lee, *SID Int. Symp. Digest of Technical Papers*, John Wiley & Sons, Inc., Vancouver, Canada **2013**.
- [11] B. Kim, H. G. Kim, G. Y. Shim, J. S. Park, K. I. Joo, D. J. Lee, J. H. Lee, J. H. Baek, B. K. Kim, Y. Choi, H. R. Kim, *Appl. Opt.* **2018**, 57, 119.
- [12] R. Manda, S. Pagidi, M. S. Kim, C. H. Park, H. S. Yoo, K. Sandeep, Y. J. Lim, S. H. Lee, *Liq. Cryst.* **2018**, 45, 736.
- [13] F. Castles, F. V. Day, S. M. Morris, D. H. Ko, D. J. Gardiner, M. M. Qasim, S. Nosheen, P. J. Hands, S. S. Choi, R. H. Friend, H. J. Coles, *Nat. Mater.* **2012**, 11, 599.
- [14] H. Choi, H. Higuchi, H. Kikuchi, *Appl. Phys. Lett.* **2011**, 98, 131905.
- [15] Y. H. Lin, H. S. Chen, H. C. Lin, Y. S. Tsou, H. K. Hsu, W. Y. Li, *Appl. Phys. Lett.* **2010**, 96, 113505.
- [16] J. H. Yu, H. S. Chen, P. J. Chen, K. H. Song, S. C. Noh, J. M. Lee, H. Ren, Y. H. Lin, S. H. Lee, *Opt. Express* **2015**, 23, 17337.
- [17] H. Ren, Y. H. Fan, Y. H. Lin, S. T. Wu, *Opt. Commun.* **2005**, 247, 101.
- [18] R. Manda, S. Pagidi, S. S. Bhattacharyya, C. H. Park, Y. J. Lim, J. S. Gwag, S. H. Lee, *Opt. Express* **2017**, 25, 24033.
- [19] J. Yan, Y. Li, S. T. Wu, *Opt. Lett.* **2011**, 36, 1404.
- [20] Y. J. Lim, J. H. Yoon, H. Yoo, S. M. Song, R. Manda, S. Pagidi, M. H. Lee, J. M. Myoung, S. H. Lee, *Opt. Mater. Express* **2018**, 8, 3698.
- [21] E. J. Shin, S. C. Noh, T. H. Kim, J. H. Kim, P. Nayek, M. H. Lee, M. S. Kim, L. C. Chien, J. H. Lee, B. K. Kim, S. H. Lee, *SID Int. Symp. Digest of Technical Papers*, John Wiley & Sons, Inc., CA, USA **2015**.
- [22] J. Kerr, *J. Sci.* **1875**, 50, 337.
- [23] J. Yan, Y. Xing, Q. Li, *Opt. Lett.* **2015**, 40, 4520.
- [24] S. Pagidi, R. Manda, Y. J. Lim, S. M. Song, H. Yoo, J. H. Woo, Y. H. Lin, S. H. Lee, *Opt. Express* **2018**, 26, 27368.
- [25] G. P. Montgomery Jr., J. L. West, W. Tamura-Lis, *J. Appl. Phys.* **1991**, 69, 1605.
- [26] M. Xu, B. Jin, R. He, H. Ren, *Opt. Express* **2016**, 24, 8142.
- [27] X. Wang, H. Ren, Q. Wang, *J. Disp. Technol.* **2016**, 12, 773.
- [28] C. Lan, Z. Zhou, H. Ren, S. Park, S. H. Lee, *J. Mol. Liq.* **2019**, 283, 155.
- [29] J. Yan, L. Rao, M. Jiao, Y. Li, H. C. Cheng, S. T. Wu, *J. Mater. Chem.* **2011**, 21, 7870.
- [30] C. M. Chang, Y. H. Lin, V. Reshetnyak, C. H. Park, R. Manda, S. H. Lee, *Opt. Express* **2017**, 25, 19807.
- [31] S. Pagidi, R. Manda, S. S. Bhattacharyya, K. J. Cho, T. H. Kim, Y. J. Lim, S. H. Lee, *Composites, Part B* **2019**, 164, 675.
- [32] H. Ren, Y. H. Lin, Y. H. Fan, S. T. Wu, *Appl. Phys. Lett.* **2005**, 86, 141110.